Journal of Orthopaedic Translation (2015) 3, 166—177

Available online at www.sciencedirect.com

ScienceDirect

journal homepage: http://ees.elsevier.com/jot

REVIEW ARTICLE

# Multimodal imaging of bone metastases: From preclinical to clinical applications

Stephan Ellmann [a,*], Michael Beck [b], Torsten Kuwert [b], Michael Uder [a], Tobias Bäuerle [a]

[a] *Institute of Radiology, University Medical Centre Erlangen, Erlangen, Germany*
[b] *Institute of Nuclear Medicine, University Medical Centre Erlangen, Erlangen, Germany*

Received 13 March 2015; received in revised form 17 June 2015; accepted 22 July 2015
Available online 13 August 2015

**KEYWORDS**
bone metastases;
computed tomography;
magnetic resonance imaging;
multimodal imaging;
positron-emission tomography;
translational research

**Summary** Metastases to the skeletal system are commonly observed in cancer patients, highly affecting the patients' quality of life. Imaging plays a major role in detection, follow-up, and molecular characterisation of metastatic disease. Thus, imaging techniques have been optimised and combined in a multimodal and multiparametric manner for assessment of complementary aspects in osseous metastases. This review summarises both application of the most relevant imaging techniques for bone metastasis in preclinical models and the clinical setting.


## Introduction

Metastases to the skeletal system are observed in up to 70% of all cancer patients [1]. In terms of breast cancer, bony metastases are in almost one third of all patients the only site of presentation at the initial diagnosis of metastatic disease [2]. Whereas overall survival of patients with breast cancer bone-only metastases is $>$ 2 years, it is drastically reduced to approximately half a year in patients with simultaneous liver metastases [3]. Patients with bone metastases of lung cancer exhibit *per se* lower overall survival measured in months [1]. Even though bone metastases are not necessarily a life-threatening component of cancer, their complications highly compromise the patients' quality of life. Complications of osseous metastases are referred to as skeletal-related events (SRE) and include pathologic fractures, spinal cord compression, and hypercalcemia leading to renal failure.

Established localised treatments of bone metastases imply surgery and external beam radiotherapy [4—6], providing pain relief and reducing SRE [5,6]. Besides chemotherapy, systemic treatment approaches include, in particular, bisphosphonates as an integral part of bone metastases management to reduce SRE and bone pain and to improve quality of life [7]. Targeted treatment options

* Corresponding author. Institute of Radiology, University Medical Centre Erlangen, Maximiliansplatz 1, 91054 Erlangen, Germany.
*E-mail address:* Stephan.Ellmann@uk-erlangen.de (S. Ellmann).

http://dx.doi.org/10.1016/j.jot.2015.07.004

such as the monoclonal antibody denosumab binding receptor activator of nuclear factor-kappa B ligand inhibitor are increasingly applied. Beside the reduction of SRE and bone pain, the newly introduced [$^{223}$Ra] dichloride for the treatment of bone metastases in castration-resistant prostate cancer showed a significant improvement in overall survival [8]. Nonetheless, these systemic treatment options have to be considered palliative in most cases [9].

The standard criteria for evaluating the course of a cancer disease are the Response Evaluation Criteria In Solid Tumours (RECIST) in their current version (1.1). These criteria are only partially applicable to bone metastases as merely lytic lesions with soft tissue components $>$ 1 cm are taken into account [10]. Objective tumour response of lytic lesions is defined as the shrinkage of the soft-tissue component of $>$ 30% measured as the largest diameter, progression with growth of $\geq$ 20% or new lesions. The only nonmorphological exception for response assessment is the appearance of new metastases with fludeoxyglucose positron emission tomography (FDG-PET) [11]. Osteoblastic lesions are considered immeasurable [10].

Further sets of criteria for the evaluation of bone metastases are the International Union against Cancer (UICC) and World Health Organisation (WHO) criteria. They have been used since the 1970s and include plain radiography (UICC) or radiography along with skeletal scintigraphy (SS, WHO). The UICC criteria are only valid for lytic lesions and distinguish between stable disease (growth of $<$ 25% or decrease by $<$ 50%), progressive disease ($>$ 25%), or new lesions, complete response (disappearance of all lesions), and partial response (shrinkage $>$ 50%) [12]. The more recent MD Anderson (MDA) criteria include plain radiography, SS, computed tomography (CT), and magnetic resonance imaging (MRI) [13]. They have been shown to be superior compared with the WHO classifications in differentiating between responders and nonresponders in terms of progression-free survival and clinical response [13]. The MDA criteria describe the same four response types as UICC, but take morphological criteria such as sclerosis or fill-in of lytic lesions and normalisation of blastic lesions into account. Partial response is thus defined by the acknowledgment of a response rather than quantification [12,14].

Irrespective of the set of criteria there is a time lag of 6–12 months for reliable radiographic evidence of response in many patients [15]. Owing to this lack of adequate imaging criteria most studies define SRE as the primary endpoint. Moreover, due to this time lag patients with bone-only disease are often excluded from clinical trials, which is undesirable as they occur frequently and cause severe symptoms. Overall, early treatment response is an important determinant of survival that can currently not be measured sufficiently in patients with predominant or exclusive bone disease [16]. Obviously there is a clinical need for accurate response criteria in terms of skeletal involvement, allowing for prediction of therapy efficacy early after treatment initiation.

This review outlines current and future directions in experimental and clinical settings of bone metastasis imaging for detection and follow-up of bone metastases, with a focus on the assessment of therapy response and molecular characterisation of osseous metastases. Major animal models currently used for investigation of skeletal metastases are summarised, including preclinical imaging modalities and techniques for this purpose. Furthermore, advantages and disadvantages of current clinical imaging modalities for skeletal metastases are reported.

## Preclinical imaging

### Animal models and clinical relevance

In order to facilitate diagnosis and follow-up of experimental bone metastases, animal models need to closely mimic the clinical situation. For this purpose, several animal models have been developed, each with a combination of distinct advantages and disadvantages.

The primary method to study breast cancer in transgenic mice has been the overexpression of oncogenes. The transgenic mice then develop tumours spontaneously. Whereas these models have the advantage of keeping the host in an immune competent state, they suffer from the fact that in the vast majority of cases bone metastases only occur rarely [17].

To efficiently mimic and investigate bone metastases, models have been developed involving transplantation of tumour cells. The most frequently used method for this purpose is the intracardiac injection of tumour cells in immune-compromised hosts leading to disseminated metastasis to multiple organs including bone, while lacking the process of cell–cell detachment and plasma intravasation of primary tumour cells. To further select for bone tropism skeletal metastases can be isolated and grown as a bone-specific sub-cell line. The above mentioned model for example has been used to develop bone-tropic sublines of MDA-MB-231 human breast cancer cells [18]. Another model utilizes an intravenous injection of tumour cells leading to lung metastases in most cases. Nonetheless, some of the tumour cells are able to escape the lungs and metastasise further to the bone or liver [19]. Bäuerle et al [20] describe a rat model relying on injection of MDA-MB-231 breast cancer cells into the superficial epigastric artery. This leads to the induction of bone metastases exclusively in the rats' hindlegs, with a tumour take rate of 93% and no further distant metastases [20].

A more direct way to induce bone metastases is to implant tumour cells into the bone marrow cavity (e.g., tibia). Such a model also skips many early steps of metastasis, but can be used to investigate the ability of tumour cells to colonise bone. Hereby, it was possible to specify important interactions between tumour cells and bone referred to as the vicious cycle [21]. This term refers to the fact that bone resorbed by tumour cells releases factors like tumour growth factor-beta (TGF-$\beta$), which in turn positively influence tumour growth and survival. Variations of this model have also been used to test agents like bisphosphonates [22] and denosumab [23].

In a so-called orthotopic transplant model, tumour cells are injected into the primary site (e.g., the mammary fat pad). This requires the cells to undergo the full process of metastasis: development of a primary tumour, intravasation, extravasation, and colonisation. As this model is preferable in terms of fully simulating the metastatic process, many tumour cell lines are not able to metastasise to

the skeleton when transplanted orthotopically for yet unknown reasons [18]. One exception is the human breast cancer 4T1 cell line, which metastasises to bone infrequently, but allowed the isolation of a highly osteotropic subline [24]. Another model describes the implantation of human bone tissue or a bone-like matrix into the flank of immune-deficient mice, followed by transplantation of human breast cancer cell lines into the mammary fat pad. In this model, the interesting case of a cell line metastasising to the transplanted human bone, but not to the mouse bones was observed, suggesting a species-specific mechanism for osteotropism [25].

All the above-mentioned models feature their specific strengths and weaknesses. Most models do not fully simulate the complete metastatic process, which can be of advantage or disadvantage, dependent on the particular aims of the study. Others rely on destruction of bone in the case of local implantation into the bone marrow and others depend on relatively time-consuming surgical procedures. For imaging purposes, however, such animal models are adequate in anticipating the location of metastasis appearance to optimise methods for early detection of lesions. For follow-up of skeletal metastases, animal models with one or few locations of metastasis are appropriate to allow for a relatively long observation period, which is hampered in diffuse metastatic disease due to ethical reasons.

Though animal models shall closely mimic the clinical situation, the potency of experimental approaches for early detection, follow-up, and characterisation of metastases is critically dependent on data acquisition and imaging. Ideal imaging modalities are quantitative, have high spatial resolution and sensitivity, can detect little tumour masses and allow for longitudinal *in vivo* imaging over longer time periods. Most promising for this purpose is the simultaneous or sequential use of complementary methods—referred to as multimodal imaging—combining the advantages of several modalities to overcome particular drawbacks of individual modalities.

## CT

Micro-CT has the advantage of high spatial resolution (as low as 10—200 μm) and rapid data acquisition within minutes. Moreover, it is cost-effective and can display the microarchitecture of bone for the determination of effects on bone structure, even in early stages of bone destruction. Furthermore, after contrast media application, CT-angiography enables visualisation and follow-up of the abundant vasculature found particularly in osteolytic lesions (Figure 1) [26—28]. Besides assessing morphology of skeletal lesions, dynamic contrast-enhanced CT (DCE-CT) allows for early treatment response assessment of anti-angiogenic therapy in an experimental breast cancer bone metastasis model [26,27].

Drawbacks include the low soft tissue contrast compared with MRI and the levels of radiation potentially high enough to induce changes in immune response and biological pathways, thus imitating radiotherapy [29]. Although radiation is more or less negligible in a one-time scan, it might turn out to a more severe problem in longitudinal studies with several imaging procedures.

## MRI

MRI offers noninvasive high spatial resolution images (as low as 50—100 μm) along with excellent soft tissue contrast. For small animal imaging μMRI units with ultrahigh magnetic fields were developed for even higher resolution. Apart from morphological imaging, functional data can be obtained including information on tissue composition, perfusion, oxygenation, elasticity, metabolism, and molecular structures (Figure 1) [28,30]. As an example of functional imaging in analogy to μCT, DCE-MRI allows for quantitative assessment of microcirculation parameters to evaluate the role of angiogenesis in skeletal metastases (Figure 1) [26—28]. In another study, mesenchymal stem cells were labelled with superparamagnetic iron oxide nanoparticles and could be traced with MRI both *in vitro* and *in vivo*, indicating that MRI can potentially be used to assess even small amounts of cells (e.g., cancer stem cells) [31].

Drawbacks, especially in small animal imaging, are movements that disturb the high spatial resolution and should be compensated for by anaesthesia and gating algorithms. Further disadvantages include the poor sensitivity in terms of molecular structures and reactions as well as relatively long acquisition times resulting in high costs [32].

## Ultrasound

Ultrasound (US) offers high spatial and temporal resolution along with good soft tissue contrast. However, it has limited depth penetration compared with MRI and CT. This issue is particularly relevant for imaging of bone metastases as penetration of US is limited by cortical bone [30]. After local destruction of bone in osteolytic lesions, US nonetheless is applicable to assess the soft tissue component of skeletal metastases and DCE-US allows for real-time imaging of vascularisation in bone metastases after intravenous injection of microbubbles [28,33].

## PET and single photon emission CT

CT and MRI provide mainly information on morphological and functional aspects of bone metastases, other modalities from nuclear medicine rather record information on tumour metabolism and molecular structures. PET is a technique detecting pairs of high energy γ-rays emitted indirectly by a positron-emitting radiotracer. Single photon emission-CT (SPECT) is very similar but uses lower energy γ-rays and traces only single radiation, thus displaying a lower sensitivity compared with PET, but offering true three-dimensional (3D) information [34]. PET and SPECT are used not to localise tumour sites but rather provide information on metabolic processes including whole-body pharmacokinetics [35].

One advantage of SPECT is that multiple molecular functions can be evaluated by the use of different energy radioisotopes. For PET, one commonly used tracer is fluorodeoxyglucose (FDG) to explore glycolysis in tumourigenesis [36]. Major drawbacks are high costs and the poor spatial resolution of 1—2 $mm^3$. This disadvantage can be

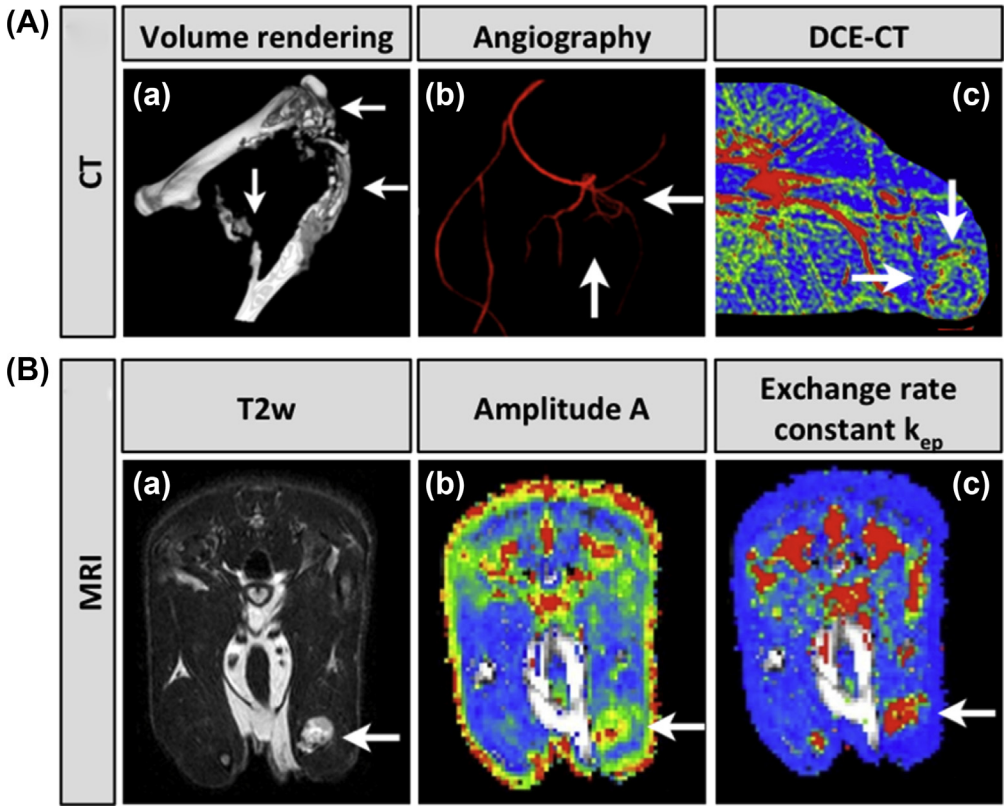


**Figure 1** (A) 3D VCT reconstructions of an osteolytic bone metastasis (a) and angiography of tumour-induced new vessel formation (b) as well as a DCE-CT colour map in axial orientation from the parameter peak enhancement (c). The colour map for DCE-CT data ranges from red (high values) to blue (low values). (B) Axial MR sections. T2w MRI (a) and DCE-MRI colour maps for amplitude A (associated with blood volume; b), exchange rate constant $k_{ep}$ (associated with vessel permeability; c). The colour map for DCE-MRI data ranges from red (high values) to blue (low values). Arrows point to bone metastases. From "Multi-modal imaging of angiogenesis in a nude rat model of breast cancer bone metastasis using magnetic resonance imaging, volumetric computed tomography and ultrasound" by T. Bäuerle et al, 2012, Journal of Visualised Experiments, 14, p. e4178. Copyright 2012, MyJoVE Corporation of 1 Alewife Center, Suite 200, Cambridge, Massachusetts 02140. Adapted with permission. 3D = 3 dimensional; CT = computed tomography; DCI = dynamic contrast-enhanced; MRI = magnetic resonance imaging; VCT = volumetric computed tomography.

overcome by combining μPET with μCT (μPET/CT). The increased sensitivity of this combination to molecular details holds several advantages over other methods, mainly the ability to estimate the activity of osteoblasts and osteoclasts within the tissue [37].

In an experimental study [$^{68}$Ga] DOTA-E-[c(RGDfK)]$_2$ was shown to be a promising novel PET tracer suitable for the imaging of αvβ3 and αvβ5 integrins which are overexpressed in bone metastases. The tracer featured rapid and specific uptake into these metastases and fast blood clearance, rendering it an interesting target for detection and follow-up of osseous metastases (Figure 2; [38]).

## Optical imaging

Optical imaging is based on the emission of light from labelled cells or probes—either bioluminescent or fluorescent light.

Bioluminescence imaging is most frequently used for tracking cancer cells and studying their distribution and activity *in vivo*. It is easy to use, cost effective, sensitive, has a high signal-to-noise ratio, and short acquisition time [39]. Bioluminescence detects photons emitted by a biochemical reaction catalysed by luciferase [34]. As luciferase genes are not natively expressed, these models rely on the use of transgenic cells with luciferase expressed under specific promoters. For example, in a model with luciferase under the control of a TGF-β-responsive promoter, activation of TGF-β during the development of bone metastases was demonstrated by increased luciferase activity [40]. Due to low-signal intensity, the technique is still restricted to small animals and remains superficial in larger objects [34].

Fluorescence imaging detects emitted light subsequent to excitation by light of a specific wavelength. Markers for this technique are fluorescent proteins or fluorochromes targeted to specific cell compartments or molecules (e.g., receptors). As tissue penetration is higher in the far-red or near-infrared, fluorescent substances have to be in these regions for deeper noninvasive imaging of small animals [41].

For optical imaging applications, Zaheer et al [42] introduced the bisphosphonate pamidronate covalently coupled to a near-infrared fluorophore, and subsequent studies proved that osteoblast activity can be monitored

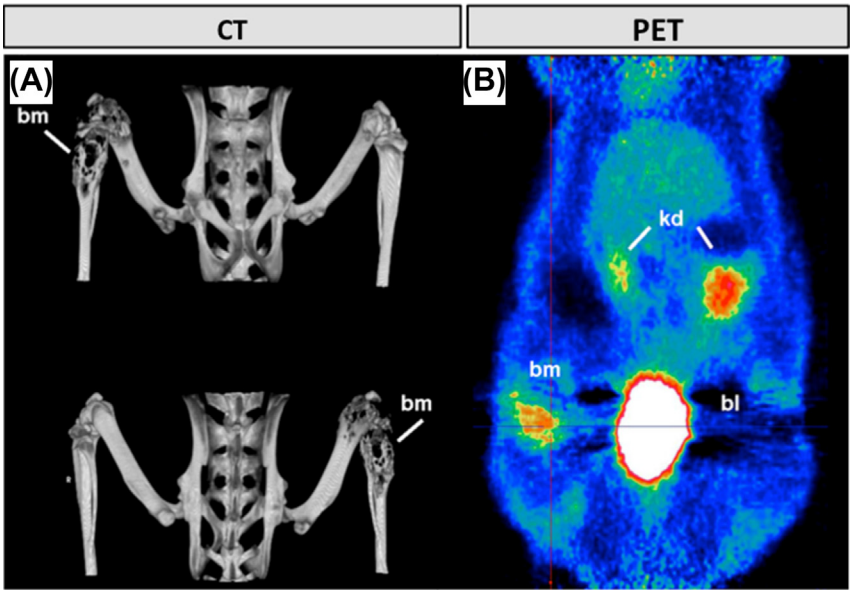


**Figure 2** (A) Three-dimensional volumetric computed tomography reconstruction of the pelvis and the hind legs of the same animal (upper reconstruction: anterior-posterior; lower reconstruction: posterior-anterior); (B) coronal μPET image (single frame) of a nude rat bearing a bone metastasis after the injection of [$^{68}$Ga] DOTA-E-[c(RGDfK)]$_2$. From "A novel PET tracer for the imaging of alphavbeta3 and alphavbeta5 integrins in experimental breast cancer bone metastases," by U. Mühlhausen et al, 2011, Contrast Media & Molecular Imaging, 6, p. 413—20. Copyright 2011, John Wiley and Sons. Reprinted with permission. Bm = bone metastasis; bl = bladder; CT = computed tomography; kd = kidneys; PET = positron emission tomography.

using near-infrared fluorophore-tagged bisphosphonate [43]. This study, moreover, employed fluorescence molecular tomography resulting in true 3D images. Additionally, several bone-specific probes have been developed commercially including fluorescently labelled bisphosphonates, which are incorporated at skeletal sites with high turnover, e.g., during cancer-induced bone remodelling [43].

Another technique referred to as quantum dots includes the coupling of fluorescent particles to antibodies, e.g., for detection of cell surface markers [44]. However, these probes tend to have high background levels due to the presence of unbound probes. A smart probe is a cleavable probe providing information on enzyme activity. The enzyme substrate is coupled to a fluorophore, which is quenched due to the close localisation of these two components. Upon cleavage, the fluorophore is released and can be detected. For example, the smart probe prosense can be used to visualize cathepsin-K activity which is significantly higher in osteolytic bone lesions and sites of resorption [43]. Other smart probes allow for visualisation of matrix metalloproteases, which are important for cancer cell motility and invasion [45], or for targeting integrins [46].

## Clinical imaging

### SS

SS is a common technique for the detection of bone metastases and has been used for decades to detect bone lesions of osteotropic tumours (e.g., breast, prostate, thyroid, and kidney cancer). SS utilizes technetium-99m bound to bisphosphonates such as methylene diphosphonate [($^{99m}$Tc) MDP], hydroxymethylene diphosphonate, or dicarboxypropane diphosphonate to visualise increased osteoblastic activity and skeletal vascularity [47]. Thus, rapid whole-body imaging for screening of metastases is feasible at relatively low costs.

For the assessment of disseminated metastatic skeletal lesions, SS was successfully applied and shown to correlate with prognosis as well as treatment response [48]. Response evaluation though is limited due to a lack of sensitivity, specificity, spatial resolution, and the delay of changes compared with clinical parameters [16]. Computer-assisted SS image analysis can optimize SS assessment by determining the percentage of positive areas in scintigraphy (%PABS). The importance of %PABS as a prognostic indicator can be seen in survival curves, in patients with $>$ 25% decline in %PABS after therapy surviving longer than those with less decline [48].

As a major drawback, lytic lesions or rapidly growing lesions with thus reduced osteoblastic activity feature little or no uptake and cannot sufficiently be assessed with SS [49]. However, increased osteoblastic activity due to the formation of new bone causes a "flare phenomenon" evident 4—12 weeks from therapy onset—this phenomenon has been described in 6—25% of patients with prostate cancer metastases and in 33% of patients with treated breast cancer metastases [50]. Whereas the flare phenomenon is rather a sign of treatment response, it might be misinterpreted as disease progression [51]. A solution to avoid misinterpretation of the flare reaction is to wait 6 months (according to MDA criteria) before evaluating a response [52], hampering the possibility of an early response assessment.

Apart from the flare reaction, other false positive SS results are obtained due to increased tracer accumulation in fractured bone, Paget's disease, or inflamed areas [53]. As an additional drawback, no information on anatomical structures adjacent to bone is retrieved with SS—e.g., it is not possible to evaluate the spinal canal in patients with vertebral metastases and the soft tissue component of bony metastases, which in many cases exceeds the size of the bony lesion.

## Conventional radiography

Conventional radiography (CR) using X-rays may be useful as a complement to SS in atypical findings, or to assess the osteolytic or osteoblastic nature of a lesion and the fracture risk, as it is able to display osteolytic lesions as areas of reduced density and osteoblastic lesions as areas of increased intensity without providing information on the tumour itself.

Whereas SS is sensitive, lesions are sufficiently visible with CR only when their bone loss exceeds 50% [12]. Signs of treatment response in metastatic lesions are the evolvement of a sclerotic rim, lesion fill-in, formation of blastic bone, or in highly responsive patients complete fading of the lesion [54]. Nonetheless, increasing bone density is seen in responding patients as well as in patients with progressing osteoblastic lesions, rendering response evaluation difficult [55]. Due to the low sensitivity of CR, changes are often not seen until 3—6 months after therapy initiation [55] and sometime even absent despite clinical improvement [14].

## CT

CT offers higher sensitivity compared with CR, as it lacks superposition of anatomical structures along with higher spatial resolution of morphological details. In addition, CT allows for 3D volume rendering and windowing to adjust bone and soft tissue contrast, which makes CT especially superior to CR in the evaluation of tumours of the spine (Figure 3) [56]. Bone metastases can be assessed in the state of bone marrow infiltration prior to evident bone destruction [57], and in more advanced disease stability and fracture risk can be evaluated [58].

As in CR, fill-in or fainting of lesions indicates therapy response, whereas an increase of the lesion size suggests disease progression.

Interestingly, it was reported that directly after completion of radiotherapy bone density decreased by 25% in 19 patients with vertebral metastases, followed by a significant increase of 61% after 3 months and reossification being accompanied by pain relief [59].

An increase in size of osteolysis in previously sclerotic lesions or an increase in soft tissue extension are reliable signs of disease progression [14]. A lack of changes or the appearance of new sclerotic lesions have to be considered more cautiously in terms of response evaluation [14].

CT is superior to CR as responses after chemotherapy and hormonal treatment of breast cancer patients with bone metastases concurred in 65% of patients with clinical parameters, whereas CR results concurred in only 35% of

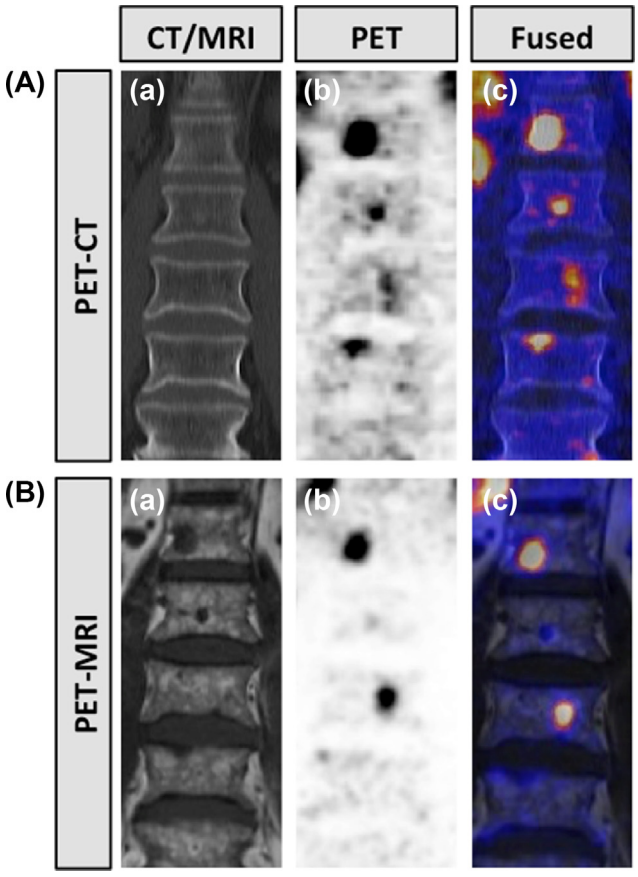


**Figure 3** Bone metastases of a neuroendocrine tumour in the thoracolumbar spine, coronal reconstructions. (A) PET-CT, with the CT component in bone window (a) exhibiting only decent sclerosis of the metastatic lesions, [$^{68}$Ga] DOTATATE PET (b) and fused image (c). (B) PET-MRI with a T2w MRI sequence (a), [$^{68}$Ga] DOTATATE PET (b) and fused image (c). Note the signal alteration of the metastases in the vertebral bodies on T2w images with different tracer uptake on PET. CT = computed tomography; MRI = magnetic resonance imaging; PET = positron emission tomography.

patients [60]. Furthermore, whole body imaging of the skeleton can be performed in a low-dose technique in a fraction of the time needed for a CR survey. Dose saving techniques, such as automatic tube current modulation, can reduce radiation exposure by 10—68% [61]. Further improvements are forthcoming by the increasing use of iterative reconstruction algorithms. Additionally, CT examinations of the thorax, abdomen, and pelvis are in many cancer patients repeatedly performed for visceral lesion detection and follow-up, thus offering a nonsuperimposed acquisition of the bones, particularly spine and pelvis.

## MRI

MRI offers a sensitivity and specificity of 70—100% for the detection of bony metastases. A meta-analysis of patients with bony metastases of breast cancer described a pooled sensitivity for MRI of 97%, significantly higher than for FDG-PET (83%) and SS (87%). The pooled specificity values for

MRI (97%) and FDG-PET (95%) were both significantly higher than for SS (88%) [62]. It is, moreover, considered at least as sensitive as CT, SS, or CR [63].

MRI is especially useful for evaluation of bone marrow infiltration [64] with excellent negative and positive predictive values [65] using T1-weighted spin-echo and fat-suppressed short tau inversion recovery sequences. Due to the high soft tissue and bone marrow contrast, MRI is superior to CT in defining soft tissue components of bony metastases [66] according to RECIST with a study leading to almost twice as many patients that could be classified via RECIST (73% vs. 37%) [67]. In terms of whole body imaging, MRI is superior to CT in staging patients with bone marrow lesions and multiple myeloma [68].

MRI, moreover, allows for the assessment of complications such as spinal cord or nerve compression with further impacts on clinical management [69]. Additionally, where pathologic fractures are an obvious sign of disease progression, benign osteoporotic fractures may also occur during the course of disease. By conventional methods, such fractures could be misinterpreted as disease progression, while MRI can prove their benign origin. The possibility of imaging cortical bone is limited due to its very short T2 relaxation time.

The application of a contrast agent along with dynamic sequences (dynamic contrast-enhanced MRI, DCE-MRI) facilitates the discrimination between viable and necrotic tumour masses. The DCE-MRI parameter amplitude-A reflects blood volume and was proven to be an early indicator of treatment response in antiangiogenic therapies, even before a change in morphology was observable [26]. Amplitude-A was moreover identified as a statistically significant variable of event-free survival in patients with multiple myeloma [70] and correlated to vessel density in histology [71]. Both DCE-MRI parameters, amplitude-A and the exchange rate reflecting vascular permeability ($k_{ep}$) were significantly higher in lesions with marked bone marrow infiltration than in lesions with mild or no infiltration [71], and $k_{ep}$ was significantly decreased in myeloma patients after antiangiogenic therapy in combination with chemotherapy [72]. DCE-MRI, however, is not relevant for the detection and whole-body assessment of metastatic disease, as anatomic coverage is limited. Furthermore, standardisation across different platforms and institutes is challenging [52].

Diffusion-weighted imaging (DWI) depends on the microscopic mobility of water. The so-called Brownian motion is resulting from thermal agitation of water molecules and is highly influenced by the cellular microenvironment of tissues. DWI has been linked to cancer aggressiveness, although the biophysical reasons for this are incompletely understood.

In terms of screening and staging, DWI featured poor specificity and a low positive predictive value for the detection of tumour involved lymph nodes and bone metastases in a study including 20 breast cancer patients [73], but proved to be superior to SS and PET in prostate cancer [74]. DWI, nonetheless, has the potential to predict responses to chemotherapy and assess treatment responses before a reduction in tumour volume becomes visible [75]. Changes in the corresponding apparent diffusion coefficient (ADC) values were shown to be early indicators of therapy response. In prostate cancer bone metastases, variations in ADC were seen 2 weeks after androgen blockade with CT, SS, and conventional MRI showing no significant differences at the same time [75]. However, a rat model of bone metastases from breast cancer showed no significant changes in ADC in treated rats compared with untreated animals [26]. A clinical study in prostate cancer patients observed an ADC increase in responders, but some lesions in both responders and progressors demonstrated an ADC decrease beyond the limits of reproducibility [50].

These inconsistent and somewhat confusing results on DWI suggest a certain heterogeneity of ADC changes possibly due to cancer subtype and composition of bone marrow, leading to a lack of specificity of DWI and emphasising the need for additional morphologic sequences [74]. In addition, more recently presented analysis methods (AC parametric response functional diffusion map) take spatial information and tumour heterogeneity into account, enable careful voxel-by-voxel follow-up of treatment-induced changes, and thus an evaluation of the proportion of tumour tissues with significant changes [76].

## SPECT

SPECT uses similar radiotracers as SS, but offers higher sensitivity due to its tomographic imaging capabilities [77]. It is thus especially useful in areas of complex anatomy or bones extensively surrounded by soft tissue such as the thoracolumbar spine or the pelvis. The main limitation of SPECT is the lack of absolute quantification compared with PET, which renders it a less favourable tool in evaluating therapy response.

## PET

As PET utilizes the uptake of positron-emitting radiopharmaceuticals, [$^{18}$F] fluoride as a nonspecific bone tracer or [$^{18}$F] FDG are mostly used to evaluate bone metastases. The mechanism of [$^{18}$F] fluoride is based on diffusion of the tracer molecule through capillaries and the formation of fluoroapatite at the bone surface in areas where remodelling is pronounced [78]. FDG is taken up by most tumours and their metastases including bone metastases with the uptake reflecting metabolic activity. For this reason, some slowly growing tumours (e.g., neuroendocrine and prostate tumours) cannot be detected by FDG. However, FDG is a convenient tracer for the detection of osteolytic metastases with little osteoblastic activity and has been shown to be superior to SS [79] and SPECT [80] in these cases, but less sensitive for osteoblastic metastases. In predominantly sclerotic prostate cancer metastases [$^{99m}$Tc] MDP-scintigraphy has been shown to be advantageous over FDG-PET [81].

An important drawback of FDG-PET is the unspecific uptake by muscle, inflammation, bowel, and blood pool activity in great vessels [82]. Other false positive results may derive from therapies involving the application of granulocyte colony-stimulating factor, e.g., during chemotherapy. The resulting increase of FDG uptake by hyperplastic bone marrow can mimic diffuse bone marrow infiltration by tumour [83]. Importantly, this interference

has not been described with [$^{18}$F] fluoride-PET, encouraging its use in patients under chemotherapy along with granulocyte colony-stimulating factor [84]. [$^{18}$F] Fluoride-PET has also been shown to detect some lytic and early marrow-based metastases [85] as well as sclerotic lesions due to prostate cancer metastases [86] that could both not be identified by [$^{99m}$Tc] MDP-SS. Nonetheless, the usage of [$^{18}$F]-FDG might be more attractive in certain situations, since uptake of this radiotracer resembles the mass of viable tumour cells, whereas [$^{18}$F] fluoride is rather reflecting the extent of bone reaction [12].

Depending on the primary tumour, some dedicated radiopharmaceuticals can be used for specific imaging as well. Concerning neuroendocrine tumours, [$^{68}$Ga] labelled peptides like DOTATOC or DOTANOC are used (Figure 3) [87]. DOTATOC however showed no advantage over conventional anatomic imaging, although it detected new metastases earlier during therapy [88].

[$^{18}$F] fluorothymidine is a biomarker reflecting cell proliferation with a good correlation between uptake in breast cancer and the Ki-67 labelling index [89]. In comparison to FDG, [$^{18}$F] fluorothymidine was shown to exhibit stronger correlation to outcomes [90] and a potentially predictive role at an even earlier time point during chemotherapy [91]. 16-alpha-[$^{18}$F] fluoroestradiol or progesterone allows for specific imaging of receptor-positive breast cancer metastases with low 16-alpha-[$^{18}$F] fluoroestradiol uptake in tumour lesions showing a strong predictive value for the failure of antihormonal therapy [92]. These results also support future trials to reassess oestrogen receptor expression in metastases in a noninvasive manner, e.g., in patients that cannot be biopsied. It is a valuable tool in differentiating between benign and malignant lesions and between metastases from different tumour types [93].

In a feasibility study in HER2-positive metastatic breast cancer patients [$^{89}$Zr] trastuzumab was proven to effectively visualise HER2-positive lesions including bone metastases [94].

Another example is the prostate-specific membrane antigen PET with a [$^{68}$Ga] labelled small molecule antagonist against the prostate specific membrane antigen. This antigen is expressed intracellularly by prostate cells but becomes extracellularly located during malignant transformation of prostate cells. The receptor density shows a positive correlation with the tumour grading leading to higher tracer uptake in dedifferentiated malignancies [95]. Compared to the established [$^{18}$F] choline PET/CT, prostate-specific membrane antigen PET/CT showed a significantly higher detection rate of prostate cancer lesions overall and also at low prostate specific antigen levels [96].

PET moreover allows for absolute quantification with the standardized uptake value (SUV) quantifying the tracer uptake of target lesions. $SUV_{max}$ in this context is the value limited to the most active voxel and is highly reproducible across observers. In breast cancer patients with disseminated bone metastases the change in pre- to posttreatment SUV values correlated strongly with both clinical response and percentage change in tumour marker value [97], with 30–54% decreased values in responding sites versus marginally or unchanged values in nonresponding lesions [98]. The parameter $K_i$ indicates regional clearance of [$^{18}$F] fluoride from blood plasma to bone mineral and was shown to be three times higher in metastatic lesions compared with adjacent unaffected bone [78]. The already described flare phenomenon following (hormonal) therapy can also be observed in PET and is an indicator of early therapy response [99].

The European Organisation for Research and Treatment of Cancer defined criteria for the quantitative assessment of metastatic lesions using PET [100]. These criteria and the PET response criteria in solid tumours [36] yield very similar results in terms of response classification of patients [101].

## Hybrid techniques

The combination of imaging techniques such as PET/CT, SPECT/CT, and PET/MRI allows for the fusion of complementary images and adds specificity to the assessment of metastatic lesions compared with either modality separately. SPECT-guided CT was able to clarify $>$ 90% of SPECT findings classified as indeterminate in an analysis that was masked as to clinical pretest probability and the planar scan findings [102]. PET/CT assessment of bone metastases revealed an increase in CT attenuation and decrease in SUV as potential predictors of early therapy response [103]. Interestingly, CT attenuation and SUV showed a significantly negative correlation. The additional benefit of hybrid imaging mainly derives from the combination of the assessment of tumour cells by PET metabolically and the assessment of bone structure by CT in a microanatomic manner (Figure 3).

Comparing [$^{18}$F] FDG PET/CT with SS, the hybrid technique was shown to be superior in evaluating bone metastases of hematologic malignancies [104], as well as head and neck cancers [105]. In a study with 39 breast cancer patients with bone metastases, overall sensitivity and specificity for [$^{18}$F] fluoride PET were 91% and 91%, respectively, compared to 77% and 93%, respectively, for CT. The integrated assessment ([$^{18}$F] fluoride PET/CT) yielded a combined sensitivity of 98% with a corresponding specificity of 93% [106]. Newly introduced methods allow for absolute quantification in SPECT/CT. Based on the CT derived attenuation correction local tracer uptake in kBq/mL and in addition body weight normalised SUV values can be calculated [107]. The published data to date regarding SS showed a high correlation to uptake measured with [$^{18}$F] fluoride PET [108].

## Conclusion and future directions

Multimodal imaging of bone metastases facilitates the assessment of various parameters and biomarkers on a morphological, functional, and molecular level. A major challenge for detection, follow-up, and molecular characterisation of skeletal metastases is the appropriate choice of imaging modality and technique, respectively.

Animal models of bone metastases are helpful for the evaluation of novel imaging techniques to be correlated with histology, which in most cases is not applicable in patients. In particular, monitoring growth of metastases longitudinally and therapy response assessment in animal models is essential for further improvement of imaging

techniques and parameters, e.g., in regard to the respective therapy mechanism. While some clinically applied imaging techniques can be back-translated for optimisation and histologic correlation in animal models, such improved imaging methods can subsequently find their way back into clinical application. Thus, preclinical modelling of metastatic skeletal disease is an important part of the development of novel and improved imaging techniques.

The most frequently applied clinical classification system for treatment response assessment is RECIST. To further improve the therapeutic response evaluation of skeletal metastases there is urgent need for inclusion of more sophisticated morphological and functional criteria, e.g., to specifically assess responses to targeted therapies. These might include quantitative measurements of bone density and MRI-derived signal intensity to improve accuracy and objectivity [109]. Moreover, metastatic bone lesions are mainly measured unidimensionally. With the increasing spatial resolution of almost all imaging techniques, in particular contemporary CT scanners offering isotropic or near isotropic resolution, lesion measurement in three dimensions, and evaluating changes in lesion volume rather than lesion diameter might provide an easy-to-apply and sensitive way for earlier detection of therapy response or failure. Further value could be added by automatic pattern and contour recognition algorithms, allowing for higher interobserver agreements in longitudinal evaluations. Regarding functional imaging, DCE-MRI and DWI are promising techniques that will need further improvements in terms of standardised data acquisition and quantification of parameters to reliably assess treatment response.

Even with modern imaging techniques, early detection of bone metastases remains challenging. Nuclear medicine techniques such as SS, SPECT, or PET are highly sensitive for this purpose, but feature major drawbacks in terms of lesion follow-up and response quantification. Therefore, for detection as well as follow-up of metastases, hybrid imaging with PET/CT or PET/MRI holds great potential as it provides quantifiable functional or metabolic parameters as well as molecular information in combination with the anatomical information provided by CT and MRI.

Concerning the choice of radiotracers [$^{18}$F] fluoride is currently very promising for this purpose due to facilitating early identification of skeletal metastatic lesions, stronger tracer accumulation in the skeletal system as compared with [$^{99m}$Tc] MDP and easy patient preparation (no limitations to diet or physical activity required and the possibility of conducting the scan regardless of glucose concentration in the blood) [110]. The recently established quantitative SPECT/CT and multimodal reconstruction algorithms have yet to be transferred into clinical routine and further studies are needed. Molecularly specific tracers allow for non-invasive assessment of receptor status in disseminated lesions as discordances between primary tumour and metastases occur in up to 40%, which necessitates therapy adjustments. Thus, guidelines advise reevaluation of receptor status in metastatic patients using biopsies, which could be performed alternatively by imaging [111].

In summary, imaging is indispensible in bone metastasis detection, follow-up, and molecular characterisation. Evaluating disseminated osseous lesions remains challenging due to the complex morphology, slow metabolism, and heterogeneity on the molecular level. These issues might be overcome by advanced and optimised imaging techniques, as well as by the suitable combination of respective modalities, in terms of multiparametric and multimodal imaging.

## Conflicts of interest

The authors have no conflicts of interest relevant to this article.

## References

[1] Coleman RE. Clinical features of metastatic bone disease and risk of skeletal morbidity. Clin Cancer Res 2006;12:S6243—9.
[2] Niikura N, Liu J, Hayashi N, Palla SL, Tokuda Y, Hortobagyi GN, et al. Retrospective analysis of antitumor effects of zoledronic acid in breast cancer patients with bone-only metastases. Cancer 2012;118:2039—47.
[3] Plunkett TA, Smith P, Rubens RD. Risk of complications from bone metastases in breast cancer. implications for management. Eur J Cancer 2000;36:476—82.
[4] Hoskin PJ. Scientific and clinical aspects of radiotherapy in the relief of bone pain. Cancer Surv 1988;7:69—86.
[5] Chow E, Harris K, Fan G, Tsao M, Sze WM. Palliative radiotherapy trials for bone metastases: a systematic review. J Clin Oncol 2007;25:1423—36.
[6] Sze WM, Shelley M, Held I, Mason M. Palliation of metastatic bone pain: single fraction versus multifraction radiotherapy — a systematic review of the randomised trials. Cochrane Database Syst Rev 2004:CD004721.
[7] Body JJ, Diel IJ, Lichinitser MR, Kreuser ED, Dornoff W, Gorbunova VA, et al. Intravenous ibandronate reduces the incidence of skeletal complications in patients with breast cancer and bone metastases. Ann Oncol 2003;14:1399—405.
[8] Hoskin P, Sartor O, O'Sullivan JM, Johannessen DC, Helle SI, Logue J, et al. Efficacy and safety of radium-223 dichloride in patients with castration-resistant prostate cancer and symptomatic bone metastases, with or without previous docetaxel use: a prespecified subgroup analysis from the randomised, double-blind, phase 3 ALSYMPCA trial. Lancet Oncol 2014;15:1397—406.
[9] Diel IJ, Solomayer EF, Bastert G. Treatment of metastatic bone disease in breast cancer: bisphosphonates. Clin Breast Cancer 2000;1:43—51.
[10] Eisenhauer EA, Therasse P, Bogaerts J, Schwartz LH, Sargent D, Ford R, et al. New response evaluation criteria in solid tumours: revised RECIST guideline (version 1.1). Eur J Cancer 2009;45:228—47.
[11] Bensch F, van Kruchten M, Lamberts LE, Schroder CP, Hospers GA, Brouwers AH, et al. Molecular imaging for monitoring treatment response in breast cancer patients. Eur J Pharmacol 2013;717:2—11.
[12] Bäuerle T, Semmler W. Imaging response to systemic therapy for bone metastases. Eur Radiol 2009;19:2495—507.
[13] Hamaoka T, Costelloe CM, Madewell JE, Liu P, Berry DA, Islam R, et al. Tumour response interpretation with new tumour response criteria vs the World Health Organisation criteria in patients with bone-only metastatic breast cancer. Br J Cancer 2010;102:651—7.
[14] Hamaoka T, Madewell JE, Podoloff DA, Hortobagyi GN, Ueno NT. Bone imaging in metastatic breast cancer. J Clin Oncol 2004;22:2942—53.

[15] Glendenning J, Cook G. Imaging breast cancer bone metastases: current status and future directions. Semin Nucl Med 2013;43:317—23.
[16] Lecouvet FE, Larbi A, Pasoglou V, Omoumi P, Tombal B, Michoux N, et al. MRI for response assessment in metastatic bone disease. Eur Radiol 2013;23:1986—97.
[17] Goldstein RH, Weinberg RA, Rosenblatt M. Of mice and (wo) men: mouse models of breast cancer metastasis to bone. J Bone Miner Res 2010;25:431—6.
[18] Kretschmann KL, Welm AL. Mouse models of breast cancer metastasis to bone. Cancer Metastasis Rev 2012;31:579—83.
[19] Kakiuchi S, Daigo Y, Tsunoda T, Yano S, Sone S, Nakamura Y. Genome-wide analysis of organ-preferential metastasis of human small cell lung cancer in mice. Mol Cancer Res 2003;1:485—99.
[20] Bäuerle T, Adwan H, Kiessling F, Hilbig H, Armbruster FP, Berger MR. Characterisation of a rat model with site-specific bone metastasis induced by MDA-MB-231 breast cancer cells and its application to the effects of an antibody against bone sialoprotein. Int J Cancer 2005;115:177—86.
[21] Juarez P, Guise TA. TGF-beta in cancer and bone: implications for treatment of bone metastases. Bone 2011;48:23—9.
[22] Mundy GR, Yoneda T, Hiraga T. Preclinical studies with zoledronic acid and other bisphosphonates: impact on the bone microenvironment. Semin Oncol 2001;28:35—44.
[23] Canon JR, Roudier M, Bryant R, Morony S, Stolina M, Kostenuik PJ, et al. Inhibition of RANKL blocks skeletal tumor progression and improves survival in a mouse model of breast cancer bone metastasis. Clin Exp Metastasis 2008;25:119—29.
[24] Lelekakis M, Moseley JM, Martin TJ, Hards D, Williams E, Ho P, et al. A novel orthotopic model of breast cancer metastasis to bone. Clin Exp Metastasis 1999;17:163—70.
[25] Kuperwasser C, Dessain S, Bierbaum BE, Garnet D, Sperandio K, Gauvin GP, et al. A mouse model of human breast cancer metastasis to human bone. Cancer Res 2005;65:6130—8.
[26] Bäuerle T, Bartling S, Berger M, Schmitt-Graff A, Hilbig H, Kauczor HU, et al. Imaging anti-angiogenic treatment response with DCE-VCT, DCE-MRI and DWI in an animal model of breast cancer bone metastasis. Eur J Radiol 2010;73:280—7.
[27] Bäuerle T, Hilbig H, Bartling S, Kiessling F, Kersten A, Schmitt-Graff A, et al. Bevacizumab inhibits breast cancer-induced osteolysis, surrounding soft tissue metastasis, and angiogenesis in rats as visualized by VCT and MRI. Neoplasia 2008;10:511—20.
[28] Bäuerle T, Komljenovic D, Berger MR, Semmler W. Multimodal imaging of angiogenesis in a nude rat model of breast cancer bone metastasis using magnetic resonance imaging, volumetric computed tomography and ultrasound. J Vis Exp 2012;14:e4178.
[29] Beckmann N, Kneuer R, Gremlich HU, Karmouty-Quintana H, Ble FX, Muller M. *In vivo* mouse imaging and spectroscopy in drug discovery. NMR Biomed 2007;20:154—85.
[30] Koba W, Kim K, Lipton ML, Jelicks L, Das B, Herbst L, et al. Imaging devices for use in small animals. Semin Nucl Med 2011;41:151—65.
[31] Hu SL, Lu PG, Zhang LJ, Li F, Chen Z, Wu N, et al. *In vivo* magnetic resonance imaging tracking of SPIO-labeled human umbilical cord mesenchymal stem cells. J Cell Biochem 2012;113:1005—12.
[32] Gross S, Piwnica-Worms D. Molecular imaging strategies for drug discovery and development. Curr Opin Chem Biol 2006;10:334—42.
[33] Merz M, Komljenovic D, Semmler W, Bäuerle T. Quantitative contrast-enhanced ultrasound for imaging antiangiogenic treatment response in experimental osteolytic breast cancer bone metastases. Invest Radiol 2012;47:422—9.
[34] van der Horst G, van der Pluijm G. Preclinical imaging of the cellular and molecular events in the multistep process of bone metastasis. Future Oncol 2012;8:415—30.
[35] Chatziioannou AF. Instrumentation for molecular imaging in preclinical research: Micro-PET and Micro-SPECT. Proc Am Thorac Soc 2005;2:533—6.
[36] Wahl RL, Herman JM, Ford E. The promise and pitfalls of positron emission tomography and single-photon emission computed tomography molecular imaging-guided radiation therapy. Semin Radiat Oncol 2011;21:88—100.
[37] Luu AN, Anez-Bustillos L, Aran S, Araiza Arroyo FJ, Entezari V, Rosso C, et al. Microstructural, densitometric and metabolic variations in bones from rats with normal or altered skeletal states. PLoS One 2013;8:e82709.
[38] Muhlhausen U, Komljenovic D, Bretschi M, Leotta K, Eisenhut M, Semmler W, et al. A novel PET tracer for the imaging of alphavbeta3 and alphavbeta5 integrins in experimental breast cancer bone metastases. Contrast Media Mol Imaging 2011;6:413—20.
[39] O'Neill K, Lyons SK, Gallagher WM, Curran KM, Byrne AT. Bioluminescent imaging: a critical tool in pre-clinical oncology research. J Pathol 2010;220:317—27.
[40] Serganova I, Moroz E, Vider J, Gogiberidze G, Moroz M, Pillarsetty N, et al. Multimodality imaging of TGFbeta signaling in breast cancer metastases. FASEB J 2009;23:2662—72.
[41] Hilderbrand SA, Weissleder R. Near-infrared fluorescence: application to in vivo molecular imaging. Curr Opin Chem Biol 2010;14:71—9.
[42] Zaheer A, Lenkinski RE, Mahmood A, Jones AG, Cantley LC, Frangioni JV. *In vivo* near-infrared fluorescence imaging of osteoblastic activity. Nat Biotechnol 2001;19:1148—54.
[43] Kozloff KM, Weissleder R, Mahmood U. Noninvasive optical detection of bone mineral. J Bone Miner Res 2007;22:1208—16.
[44] Jaiswal JK, Mattoussi H, Mauro JM, Simon SM. Long-term multiple color imaging of live cells using quantum dot bioconjugates. Nat Biotechnol 2003;21:47—51.
[45] Bremer C, Tung CH, Weissleder R. *In vivo* molecular target assessment of matrix metalloproteinase inhibition. Nat Med 2001;7:743—8.
[46] Snoeks TJ, Khmelinskii A, Lelieveldt BP, Kaijzel EL, Lowik CW. Optical advances in skeletal imaging applied to bone metastases. Bone 2011;48:106—14.
[47] Krasnow AZ, Hellman RS, Timins ME, Collier BD, Anderson T, Isitman AT. Diagnostic bone scanning in oncology. Semin Nucl Med 1997;27:107—41.
[48] Yahara J, Noguchi M, Noda S. Quantitative evaluation of bone metastases in patients with advanced prostate cancer during systemic treatment. BJU Int 2003;92:379—83. discussion 383—4.
[49] Woolfenden JM, Pitt MJ, Durie BG, Moon TE. Comparison of bone scintigraphy and radiography in multiple myeloma. Radiology 1980;134:723—8.
[50] Messiou C, Collins DJ, Giles S, de Bono JS, Bianchini D, de Souza NM. Assessing response in bone metastases in prostate cancer with diffusion weighted MRI. Eur Radiol 2011;21:2169—77.
[51] Levenson RM, Sauerbrunn BJ, Bates HR, Newman RD, Eddy JL, Ihde DC. Comparative value of bone scintigraphy and radiography in monitoring tumor response in systemically treated prostatic carcinoma. Radiology 1983;146:513—8.
[52] Lecouvet FE, Talbot JN, Messiou C, Bourguet P, Liu Y, de Souza NM, et al. Monitoring the response of bone metastases to treatment with Magnetic Resonance Imaging and nuclear medicine techniques: a review and position statement by the European Organisation for Research and Treatment of Cancer imaging group. Eur J Cancer 2014;50:2519—31.

[53] Citrin DL. Problems and limitations of bone scanning with the 99Tcm-phosphates. Clin Radiol 1977;28:97—105.
[54] Libshitz HI, Hortobagyi GN. Radiographic evaluation of therapeutic response in bony metastases of breast cancer. Skeletal Radiol 1981;7:159—65.
[55] Vinholes J, Coleman R, Eastell R. Effects of bone metastases on bone metabolism: implications for diagnosis, imaging and assessment of response to cancer treatment. Cancer Treat Rev 1996;22:289—331.
[56] Sundaram M, McGuire MH. Computed tomography or magnetic resonance for evaluating the solitary tumor or tumor-like lesion of bone? Skeletal Radiol 1988;17:393—401.
[57] Helms CA, Cann CE, Brunelle FO, Gilula LA, Chafetz N, Genant HK. Detection of bone-marrow metastases using quantitative computed tomography. Radiology 1981;140: 745—50.
[58] Poitout D, Gaujoux G, Lempidakis M, O'Zoux P, Filippi C, Dulac P, et al. X-ray computed tomography or MRI in the assessment of bone tumor extension. Chirurgie 1991;117: 488—90.
[59] Reinbold WD, Wannenmacher M, Hodapp N, Adler CP. Osteodensitometry of vertebral metastases after radiotherapy using quantitative computed tomography. Skeletal Radiol 1989;18:517—21.
[60] Bellamy EA, Nicholas D, Ward M, Coombes RC, Powles TJ, Husband JE. Comparison of computed tomography and conventional radiology in the assessment of treatment response of lytic bony metastases in patients with carcinoma of the breast. Clin Radiol 1987;38:351—5.
[61] Mulkens TH, Bellinck P, Baeyaert M, Ghysen D, Van Dijck X, Mussen E, et al. Use of an automatic exposure control mechanism for dose optimization in multi-detector row CT examinations: clinical evaluation. Radiology 2005;237: 213—23.
[62] Liu T, Cheng T, Xu W, Yan WL, Liu J, Yang HL. A meta-analysis of 18FDG-PET, MRI and bone scintigraphy for diagnosis of bone metastases in patients with breast cancer. Skeletal Radiol 2011;40:523—31.
[63] Lecouvet FE, Geukens D, Stainier A, Jamar F, Jamart J, d'Othee BJ, et al. Magnetic resonance imaging of the axial skeleton for detecting bone metastases in patients with high-risk prostate cancer: diagnostic and cost-effectiveness and comparison with current detection strategies. J Clin Oncol 2007;25:3281—7.
[64] Imamura F, Kuriyama K, Seto T, Hasegawa Y, Nakayama T, Nakamura S, et al. Detection of bone marrow metastases of small cell lung cancer with magnetic resonance imaging: early diagnosis before destruction of osseous structure and implications for staging. Lung Cancer 2000;27:189—97.
[65] Schmidt GP, Baur-Melnyk A, Haug A, Heinemann V, Bauerfeind I, Reiser MF, et al. Comprehensive imaging of tumor recurrence in breast cancer patients using whole-body MRI at 1.5 and 3 T compared to FDG-PET-CT. Eur J Radiol 2008;65:47—58.
[66] Petren-Mallmin M, Andreasson I, Nyman R, Hemmingsson A. Detection of breast cancer metastases in the cervical spine. Acta Radiol 1993;34:543—8.
[67] Tombal B, Rezazadeh A, Therasse P, Van Cangh PJ, Vande Berg B, Lecouvet FE. Magnetic resonance imaging of the axial skeleton enables objective measurement of tumor response on prostate cancer bone metastases. Prostate 2005;65: 178—87.
[68] Baur-Melnyk A, Buhmann S, Becker C, Schoenberg SO, Lang N, Bartl R, et al. Whole-body MRI versus whole-body MDCT for staging of multiple myeloma. AJR Am J Roentgenol 2008;190:1097—104.
[69] Engelhard K, Hollenbach HP, Wohlfart K, von Imhoff E, Fellner FA. Comparison of whole-body MRI with automatic moving table technique and bone scintigraphy for screening for bone metastases in patients with breast cancer. Eur Radiol 2004;14:99—105.
[70] Hillengass J, Wasser K, Delorme S, Kiessling F, Zechmann C, Benner A, et al. Lumbar bone marrow microcirculation measurements from dynamic contrast-enhanced magnetic resonance imaging is a predictor of event-free survival in progressive multiple myeloma. Clin Cancer Res 2007;13:475—81.
[71] Nosas-Garcia S, Moehler T, Wasser K, Kiessling F, Bartl R, Zuna I, et al. Dynamic contrast-enhanced MRI for assessing the disease activity of multiple myeloma: a comparative study with histology and clinical markers. J Magn Reson Imaging 2005;22:154—62.
[72] Wasser K, Moehler T, Nosas-Garcia S, Rehm C, Bartl R, Goldschmidt H, et al. Correlation of MRI and histopathology of bone marrow in patients with multiple myeloma. Rofo 2005;177:1116—22.
[73] Heusner TA, Kuemmel S, Koeninger A, Hamami ME, Hahn S, Quinsten A, et al. Diagnostic value of diffusion-weighted magnetic resonance imaging (DWI) compared to FDG PET/CT for whole-body breast cancer staging. Eur J Nucl Med Mol Imaging 2010;37:1077—86.
[74] Lecouvet FE, Vande Berg BC, Malghem J, Omoumi P, Simoni P. Diffusion-weighted MR imaging: adjunct or alternative to T1-weighted MR imaging for prostate carcinoma bone metastases? Radiology 2009;252:624.
[75] Lee KC, Sud S, Meyer CR, Moffat BA, Chenevert TL, Rehemtulla A, et al. An imaging biomarker of early treatment response in prostate cancer that has metastasized to the bone. Cancer Res 2007;67:3524—8.
[76] Reischauer C, Froehlich JM, Koh DM, Graf N, Padevit C, John H, et al. Bone metastases from prostate cancer: assessing treatment response by using diffusion-weighted imaging and functional diffusion maps—initial observations. Radiology 2010;257:523—31.
[77] Collier Jr BD, Hellman RS, Krasnow AZ. Bone SPECT. Semin Nucl Med 1987;17:247—66.
[78] Hawkins RA, Choi Y, Huang SC, Hoh CK, Dahlbom M, Schiepers C, et al. Evaluation of the skeletal kinetics of fluorine-18-fluoride ion with PET. J Nucl Med 1992;33:633—42.
[79] Cook GJ, Houston S, Rubens R, Maisey MN, Fogelman I. Detection of bone metastases in breast cancer by 18FDG PET: differing metabolic activity in osteoblastic and osteolytic lesions. J Clin Oncol 1998;16:3375—9.
[80] Even-Sapir E, Metser U, Mishani E, Lievshitz G, Lerman H, Leibovitch I. The detection of bone metastases in patients with high-risk prostate cancer: 99mTc-MDP Planar bone scintigraphy, single- and multi-field-of-view SPECT, 18F-fluoride PET, and 18F-fluoride PET/CT. J Nucl Med 2006;47: 287—97.
[81] Shreve PD, Grossman HB, Gross MD, Wahl RL. Metastatic prostate cancer: initial findings of PET with 2-deoxy-2-[F-18] fluoro-D-glucose. Radiology 1996;199:751—6.
[82] Moon DH, Maddahi J, Silverman DH, Glaspy JA, Phelps ME, Hoh CK. Accuracy of whole-body fluorine-18-FDG PET for the detection of recurrent or metastatic breast carcinoma. J Nucl Med 1998;39:431—5.
[83] Sugawara Y, Fisher SJ, Zasadny KR, Kison PV, Baker LH, Wahl RL. Preclinical and clinical studies of bone marrow uptake of fluorine-1-fluorodeoxyglucose with or without granulocyte colony-stimulating factor during chemotherapy. J Clin Oncol 1998;16:173—80.
[84] Avery R, Kuo PH. 18F sodium fluoride PET/CT detects osseous metastases from breast cancer missed on FDG PET/CT with marrow rebound. Clin Nucl Med 2013;38:746—8.
[85] Li Y, Schiepers C, Lake R, Dadparvar S, Berenji GR. Clinical utility of (18)F-fluoride PET/CT in benign and malignant bone diseases. Bone 2012;50:128—39.

[86] Mick CG, James T, Hill JD, Williams P, Perry M. Molecular imaging in oncology: (18)F-sodium fluoride PET imaging of osseous metastatic disease. AJR Am J Roentgenol 2014;203:263—71.
[87] Koukouraki S, Strauss LG, Georgoulias V, Eisenhut M, Haberkorn U, Dimitrakopoulou-Strauss A. Comparison of the pharmacokinetics of 68Ga-DOTATOC and [18F]FDG in patients with metastatic neuroendocrine tumours scheduled for 90Y-DOTATOC therapy. Eur J Nucl Med Mol Imaging 2006;33:1115—22.
[88] Gabriel M, Oberauer A, Dobrozemsky G, Decristoforo C, Putzer D, Kendler D, et al. 68Ga-DOTA-Tyr3-octreotide PET for assessing response to somatostatin-receptor-mediated radionuclide therapy. J Nucl Med 2009;50:1427—34.
[89] Smyczek-Gargya B, Fersis N, Dittmann H, Vogel U, Reischl G, Machulla HJ, et al. PET with [18F]fluorothymidine for imaging of primary breast cancer: a pilot study. Eur J Nucl Med Mol Imaging 2004;31:720—4.
[90] Pio BS, Park CK, Pietras R, Hsueh WA, Satyamurthy N, Pegram MD, et al. Usefulness of 3′-[F-18]fluoro-3′-deoxythymidine with positron emission tomography in predicting breast cancer response to therapy. Mol Imaging Biol 2006;8:36—42.
[91] Kenny L, Coombes RC, Vigushin DM, Al-Nahhas A, Shousha S, Aboagye EO. Imaging early changes in proliferation at 1 week post chemotherapy: a pilot study in breast cancer patients with 3′-deoxy-3′-[18F]fluorothymidine positron emission tomography. Eur J Nucl Med Mol Imaging 2007;34:1339—47.
[92] Linden HM, Stekhova SA, Link JM, Gralow JR, Livingston RB, Ellis GK, et al. Quantitative fluoroestradiol positron emission tomography imaging predicts response to endocrine treatment in breast cancer. J Clin Oncol 2006;24:2793—9.
[93] McGuire WL, Chamness GC, Fuqua SA. Estrogen receptor variants in clinical breast cancer. Mol Endocrinol 1991;5:1571—7.
[94] Dijkers EC, Oude Munnink TH, Kosterink JG, Brouwers AH, Jager PL, de Jong JR, et al. Biodistribution of 89Zr-trastuzumab and PET imaging of HER2-positive lesions in patients with metastatic breast cancer. Clin Pharmacol Ther 2010;87:586—92.
[95] Eder M, Eisenhut M, Babich J, Haberkorn U. PSMA as a target for radiolabelled small molecules. Eur J Nucl Med Mol Imaging 2013;40:819—23.
[96] Afshar-Oromieh A, Zechmann CM, Malcher A, Eder M, Eisenhut M, Linhart HG, et al. Comparison of PET imaging with a (68)Ga-labelled PSMA ligand and (18)F-choline-based PET/CT for the diagnosis of recurrent prostate cancer. Eur J Nucl Med Mol Imaging 2014;41:11—20.
[97] Stafford SE, Gralow JR, Schubert EK, Rinn KJ, Dunnwald LK, Livingston RB, et al. Use of serial FDG PET to measure the response of bone-dominant breast cancer to therapy. Acad Radiol 2002;9:913—21.
[98] Gwak HS, Youn SM, Chang U, Lee DH, Cheon GJ, Rhee CH, et al. Usefulness of (18)F-fluorodeoxyglucose PET for radiosurgery planning and response monitoring in patients with recurrent spinal metastasis. Minim Invasive Neurosurg 2006;49:127—34.
[99] Dehdashti F, Flanagan FL, Mortimer JE, Katzenellenbogen JA, Welch MJ, Siegel BA. Positron emission tomographic assessment of "metabolic flare" to predict response of metastatic breast cancer to antiestrogen therapy. Eur J Nucl Med 1999;26:51—6.
[100] Young H, Baum R, Cremerius U, Herholz K, Hoekstra O, Lammertsma AA, et al. Measurement of clinical and subclinical tumour response using [18F]-fluorodeoxyglucose and positron emission tomography: review and 1999 EORTC recommendations. European Organization for Research and Treatment of Cancer (EORTC) PET Study Group. Eur J Cancer 1999;35:1773—82.
[101] Thacker CA, Weiss GJ, Tibes R, Blaydorn L, Downhour M, White E, et al. 18-FDG PET/CT assessment of basal cell carcinoma with vismodegib. Cancer Med 2012;1:230—6.
[102] Romer W, Nomayr A, Uder M, Bautz W, Kuwert T. SPECT-guided CT for evaluating foci of increased bone metabolism classified as indeterminate on SPECT in cancer patients. J Nucl Med 2006;47:1102—6.
[103] Tateishi U, Gamez C, Dawood S, Yeung HW, Cristofanilli M, Macapinlac HA. Bone metastases in patients with metastatic breast cancer: morphologic and metabolic monitoring of response to systemic therapy with integrated PET/CT. Radiology 2008;247:189—96.
[104] Banwait R, O'Regan K, Campigotto F, Harris B, Yarar D, Bagshaw M, et al. The role of 18F-FDG PET/CT imaging in Waldenstrom macroglobulinemia. Am J Hematol 2011;86:567—72.
[105] Chan SC, Wang HM, Ng SH, Hsu CL, Lin YJ, Lin CY, et al. Utility of 18F-fluoride PET/CT and 18F-FDG PET/CT in the detection of bony metastases in heightened-risk head and neck cancer patients. J Nucl Med 2012;53:1730—5.
[106] Piccardo A, Altrinetti V, Bacigalupo L, Puntoni M, Biscaldi E, Gozza A, et al. Detection of metastatic bone lesions in breast cancer patients: fused (18)F-Fluoride-PET/MDCT has higher accuracy than MDCT. Preliminary experience. Eur J Radiol 2012;81:2632—8.
[107] Zeintl J, Vija AH, Yahil A, Hornegger J, Kuwert T. Quantitative accuracy of clinical 99mTc SPECT/CT using ordered-subset expectation maximization with 3-dimensional resolution recovery, attenuation, and scatter correction. J Nucl Med 2010;51:921—8.
[108] Cachovan M, Vija AH, Hornegger J, Kuwert T. Quantification of 99mTc-DPD concentration in the lumbar spine with SPECT/CT. EJNMMI Res 2013;3:45.
[109] Vassiliou V, Andreopoulos D. Assessment of therapeutic response in patients with metastatic skeletal disease: suggested modifications for the MDA response classification criteria. Br J Cancer 2010;103:925—6. author reply 927.
[110] Tarnawska-Pierscinska M, Holody L, Braziewicz J, Krolicki L. Bone metastases diagnosis possibilities in studies with the use of 18F-NaF and 18F-FDG. Nucl Med Rev Cent East Eur 2011;14:105—8.
[111] Simmons C, Miller N, Geddie W, Gianfelice D, Oldfield M, Dranitsaris G, et al. Does confirmatory tumor biopsy alter the management of breast cancer patients with distant metastases? Ann Oncol 2009;20:1499—504.